ARTICLES

Two-Dimensional Self-Diffusion of Alkylammonium Ions Located in the Interlayer Space of Tetrasilicicfluormica

Miho Yamauchi,* Shin'ichi Ishimaru, and Ryuichi Ikeda

Department of Chemistry, University of Tsukuba, Tennodai 1-1-1, Tsukuba, Ibaraki 305-8571, Japan

Received: June 30, 2003; In Final Form: November 10, 2003

A layered clay mineral, tetrasilicicfluormica intercalated with spherical, planar, and rodlike alkylammonium ions, was prepared. Two-dimensional dynamic properties of intercalated ions were investigated by solid-state ^{1}H and ^{2}H NMR and electrical conductivity measurements. From these measurements, all intercalation compounds were revealed to show two-dimensional (2-D) cationic self-diffusion between mica layers. The 2-D self-diffusion could be characterized by comparing shapes of intercalated ions and their occupancies in the interlayer space. The activation energies for the 2-D self-diffusion in the present intercalation compounds were found to be smaller than those for three-dimensional cationic diffusion in bulk crystals.

1. Introduction

Inorganic−organic nanocomposites have recently attracted attention owing to many applications to a wide range in material science,[1] such as dielectric layers, rheological reagents, reinforced plastics, and catalysis. The prominent functions of nanocomposites are closely connected to low-dimensional structures, specific orientations, and dynamic properties of intercalated organic cations.

Cationic arrangements in the interlayer space have been studied and shown to depend on the cation exchange capacity (CEC) of the clay. In tetrasilicicfluormica, with a small CEC, *n*-alkylammonium ions are placed with their long axis parallel to layers of tetrasilicicfluormica, as shown in Figure 1a.[2] On the other hand, in vermiculite with a large CEC, molecular axes in alkylammonium ions are tilted to the layers with certain angles,[3] as shown in Figure 1c. In these two-dimensional (2-D) systems, intercalated cations are expected to exhibit characteristic motions of a 2-D nature. However, these 2-D molecular dynamics have been little studied for organic cations in the interlayer space.

In this study, we have investigated the 2-D motional state of intercalated cations by solid-state NMR and ac conductivity measurements to clarify influences of the cationic shapes and sizes on dynamic properties of intercalated organic cations. To observe dynamics of intercalated ions of various shapes, we selected a platelike trimethylammonium ion, a nearly spherical tetramethylammonium ion, and chainlike *n*-butylammonium and tetramethylenediammonium ions.

2. Experimental Section

n-Butylammonium chloride and tetramethylenediammonium dichloride were prepared by neutralizing ethanol solutions of *n*-butylamine and tetramethylenediamine, respectively, with hydrochloric acid diluted with ethanol by 1:1. Commercial reagents of trimethylammonium chloride and tetramethylammonium chloride were used without further purification.

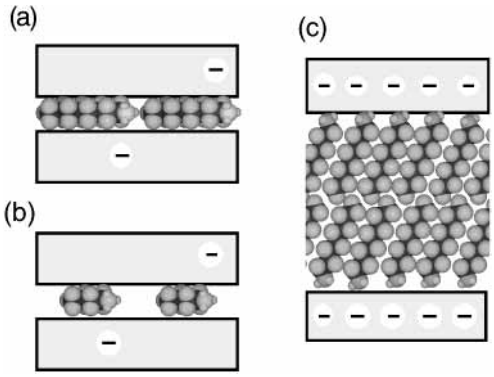

Figure 1. Structural schemes of organoclays: (a) *n*-octylammonium and (b) *n*-butylammonium ions intercalated in tetrasilicicfluormica and (c) *n*-octylammonium ions in vermiculite.

We used synthetic sodium tetrasilicicfluormica, abbreviated as Na−MC (CO-OP Chemical Co. Ltd.), which was produced from natural clay and is expressed by the ideal formula of $Na_{2x}Mg_{3-x}Si_4O_{10}F_2$ ($x = 0.3$) with a CEC of 70−80 mequiv/100 g. Intercalations of the organic cations into tetrasilicicfluormica were performed by adding Na−MC into aqueous solutions of the above ammonium salts with a concentration twice the CEC of Na−MC and stirring the mixtures for 2 days. The intercalation compounds were filtered and washed until the $AgNO_3$ test became negative. The mica specimens with trimethylammonium, tetramethylammonium, *n*-butylammonium, and tetramethylenediammonium ions are hereafter abbreviated to M3−MC, M4−MC, C41−MC, and C42−MC, respectively. The deuteration of ammonium groups in intercalated cations was carried out by keeping dried specimens in the saturated vapor of 99.5 at. % heavy water (Aldrich) for 2 days. Deuterated

* Corresponding author. Present address: Department of Chemistry, Faculty of Sciences, Kyushu University, 6-10-1 Hakozaki, Higashi-ku, Fukuoka 812-8581, Japan. E-mail: mhyamascc@mbox.nc.kyushu-u.ac.jp.

10.1021/jp035874x CCC: $27.50
Published on Web 01/07/2004

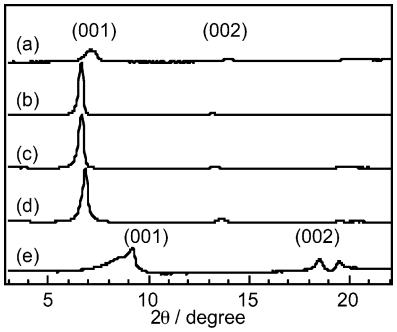

Figure 2. Powder X-ray diffraction patterns measured at 400 K in (a) $(CH_3)_3NH-MC$ (M3−MC), (b) $(CH_3)_4N-MC$ (M4−MC), (c) $CH_3-(CH_2)_3NH_3-MC$ (C41−MC), (d) $NH_3(CH_2)_4NH_3-MC$ (C42−MC), and (e) Na−MC.

TABLE 1: Interlayer Distances Calculated by Subtracting the Layer Thickness 0.96 nm from Respective *d*(001) Spacings

sample	interlayer distance/nm
M3−MC	0.28 ± 0.05
M4−MC	0.37 ± 0.03
C41−MC	0.37 ± 0.03
C42−MC	0.32 ± 0.03

M3−MC, C41−MC, and C42−MC were named M3d−MC, C41d_3−MC, and C42d_6−MC, respectively.

Powder X-ray diffraction measurements were performed with a PHILIPS X'pert PW 3040 diffractometer using Cu Kα radiation. The data were collected at 400 ± 2 K to exclude the influence of water absorbed in the interlayer space.

^{2}H NMR spectra were taken for M3d−MC, C41d_3−MC, and C42d_6−MC with a Bruker MSL-300 NMR system at a Larmor frequency of 46.1 MHz using the quadrupole-echo method[4] in the temperature range 125−440 K. The temperature dependence of ^{1}H NMR spin−lattice relaxation time (T_1) was measured at 25.7−54.4 MHz with a homemade apparatus,[5] using the $180-\tau-90°$ pulse sequence in the range 100−440 K.

Electrical conductivity measurements were performed with pellets of samples using an HP 4261A LCR meter at 1 kHz. To remove water, prepared pellets were dried in vacuo at ca. 400 K for 2 h.

3. Results and Discussion

3.1. Arrangements of Alkylammonium Ions in the Interlayer Space. X-ray powder diffraction patterns of Na−MC and the prepared intercalated compounds are shown in Figure 2. Interlayer distances in samples were estimated by subtracting the layer thickness of 0.96 nm in Na−MC[6] from basal spacings obtained from (001) reflections and are listed in Table 1. Determined interlayer distances in intercalated compounds became wider than that in Na−MC, indicating that organic cations are intercalated between clay sheets. Judging from these interlayer distance and cationic sizes, we can expect that cationic monolayers are formed between inorganic clay layers in all compounds. As for a planar trimethylammonium cation in M3−MC, its molecular plane is oriented parallel to the clay layers.

From elemental analysis of C, N, and H, we evaluated the content of intercalated ions in the specimens and the area fraction of the clay layer covered with intercalated ions by assuming van der Waals radii of respective atoms. The estimated values are shown in Table 2 together with that of *n*-octylammonium−tetrasilicicfluormica (C81−MC).[7] Area fractions obtained in M3−MC, M4−MC, and C41−MC are nearly half that obtained in C81−MC, implying that the present cations are less densely packed in interlayer spaces, as shown in Figure 1b. The small area fraction obtained in C42−MC implies that tetramethylenediammonium ions are much separated from each other compared with the other monovalent cations.

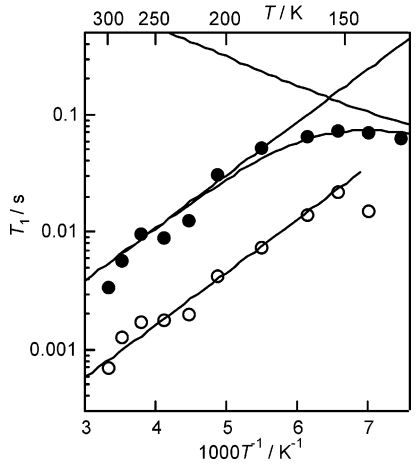

Figure 3. ^{1}H NMR spin−lattice relaxation times T_1 observed at 54.4 MHz in $(CH_3)_3NH-MC$ (M3−MC). Open and filled circles correspond to the shortest and longest T_1 values, respectively. The dotted and broken solid lines indicate calculated T_1 values for models of the cationic C_3-rotation and the cationic self-diffusion, respectively, and their superposition of the long components is given in a solid line.

TABLE 2: Area Fractions of the Clay Layer Covered with Intercalated Ions Estimated by Using van der Waals Radii of Respective Atoms

sample	fraction/%
M3−MC	71
M4−MC	67
C41−MC	77
C42−MC	43
C81−MC	130

3.2. Motional States of Alkylammonium Ions in the Interlayer Space. *3.2.1. Trimethylammonium Ions in M3−MC.* ^{2}H NMR spectra for M3d−MC showed a typical Pake pattern and no marked line shape change in the temperature range 300−420 K. A quadrupole coupling constant (QCC) of 155 ± 5 kHz evaluated from all ^{2}H spectra observed was close to 173 kHz reported for the rigid ND_3^+ group in ethylammonium chloride.[8] This implies that the molecular C_3-axis is fixed in the interlayer space and its direction has no marked fluctuation up to 420 K.

In the ^{1}H NMR T_1 measurement of M3−MC, the largest part of the recovery of the ^{1}H magnetization was fitted with a single-exponential curve below ca. 140 K. On the other hand, the recovery above 150 K showed the presence of a distributed relaxation time. We evaluated the range of T_1 by giving the shortest and the longest T_1 components. The temperature dependence of the longest and shortest values of the T_1 range is shown in Figure 3. The observed T_1 implies the presence of two relaxation processes which contribute to the relaxation above ca. 150 K. Moreover, the percentage of the short T_1 component increased with temperature, which will be discussed in the section on M4−MC.

From the measurement of the ^{1}H NMR second moment (M_2), a constant M_2 of 1.5 ± 0.2 G^2 was obtained in the range 110−300 K. The M_2 value was calculated to be 1.11 G^2 for reorientations of three CH_3 groups (CH_3-rot) and the whole cation around its C_3-axis (cation-rot).[9] Since the calculated 1.11 G^2 corresponds to the observed 1.5 G^2, the excitation of both motional modes is expected at 110 K. From this consideration, the relaxation below 150 K is attributable to cation-rot which

TABLE 3: Activation Energies for Cationic 2-D Self-Diffusion Obtained from ^{1}H NMR T_1 and Electrical Conductivity Measurements

	E_a/kJ mol^{-1}	
sample	NMR	conductivity
M3−MC	8.6 ± 0.8	13 ± 0.3
M4−MC	19 ± 5	28 ± 0.8
C41−MC	18 ± 4	25 ± 0.3
C42−MC	15 ± 2	31 ± 0.3

is usually excited at higher temperature than that observed for CH_3-rot. For these motional process, T_1 can be expressed as a BPP-type theoretical curve[10] given by

$$\frac{1}{T_1^{\mathrm{BPP}}} = \frac{2}{3}\gamma^2 \Delta M_2 \left\{ \frac{\tau}{1+\omega_0^2\tau^2} + \frac{4\tau}{1+4\omega_0^2\tau^2} \right\} \quad (1)$$

$$\tau = \tau_0 \exp\left(\frac{E_a}{RT}\right) \quad (2)$$

where γ, ΔM_2, ω_0, τ_0, and E_a are the gyromagnetic ratio of a proton, the difference in M_2 before and after the onset of the motion, the angular Larmor frequency of a proton, the motional correlation time in the limit of the infinite temperature, and the activation energy of the motion, respectively. In the limit of the fast motion, we have $\omega\tau_0 \ll 1$ and obtain a linear relation between ln T_1 and T^{-1}. From the slope of ln T_1, E_a of 13 ± 2 kJ mol^{-1} was estimated for cation-rot.

Above 150 K, T_1 values decreased with temperature and became 0.7 and 3.5 ms at 300 K. Such short T_1 values at a Larmor frequency of 54.4 MHz cannot be attributed to any fluctuations of the ^{1}H−^{1}H dipolar interactions in the present system. We assigned this relaxation mechanism above 150 K to paramagnetic impurities.[10] To observe the existence of paramagnetic species in the host clay, we carried out ESR and X-ray fluorescence measurements for Na−MC and found paramagnetic spins attributable to Fe^{3+} ions with a concentration of 0.16 wt %. This seems to originate from the natural clay used for preparing Na−MC. The estimated Fe content corresponds to 1 Fe atom per 30 nm^2 of the interlayer area where approximately 85 trimethylammonium ions are intercalated. We, accordingly, presume that the dominant process of the T_1 decrease above 150 K is the fluctuation of magnetic dipolar interactions between ^{1}H and electron spins. The fluctuation is caused by the cationic self-diffusion in the 2-D space (2-D diffusion) because paramagnetic Fe^{3+} sites are fixed in clays. In this case, ^{1}H T_1 induced by paramagnetic spins (T_1^{PARA}) is expected to be given by an analogous expression like Solomon's equation,[11] which is applicable to the relaxation from diffusional motions in a three-dimensional (3-D) system. In the limit of the slow motion, we can approximately obtain a relationship given by

$$\frac{1}{T_1^{\mathrm{PARA}}} \propto \frac{\gamma_I^2 \gamma_S^2 \hbar^2}{\langle R^6 \rangle_{\mathrm{av}}} \frac{1}{\tau} \quad (3)$$

where γ_I (γ_S), R, and $\langle R^6 \rangle_{\mathrm{av}}$ are gyromagnetic ratios of a proton (an electron), the distance between a proton and a paramagnetic site, and the time-averaged value of R^6, respectively. The observed longest and shortest T_1 values were approximately fitted by eqs 2 and 3 using the same value of E_a for the cationic 2-D self-diffusion, and the estimated E_a is shown in Table 3.

3.2.2. Tetramethylammonium Ions in M4−MC. The ^{1}H magnetization recovery for M4−MC observed above room temperature showed distributed T_1 values attributable to the presence of paramagnetic impurities in the wall by the same reason mentioned above. We estimated the range of T_1 as given in M3−MC. The temperature dependence of T_1 is shown in Figure 4. A deep minimum observed at ca. 200 K in the long T_1 could be fitted with eqs 1 and 2. Since ΔM_2 of 15 ± 1 G^2 obtained by the fitting is close to 18.9 G^2 calculated for the C_3-rotation of all methyl groups in a cation,[9] this T_1 minimum is attributable to this motion. Above 350 K, T_1 values began to decrease. From the analogous T_1 analysis in M3−MC, this T_1 decrease was attributed to the onset of the cationic 2-D self-diffusion, and the estimated activation energy is shown in Table 3. The fraction of the short T_1 component increased above 200 K and became major above ca. 350 K, as shown in Figure 4. An analogous increase was observed in M3−MC. These results indicate that the environment around intercalated cations is quite inhomogeneous in the slow-motion limit at low temperatures, while it becomes homogeneous following the frequent occurrence of cationic diffusion with increasing temperature. In the fast-motion limit at high temperatures, therefore, all protons are expected to have uniform T_1 values.

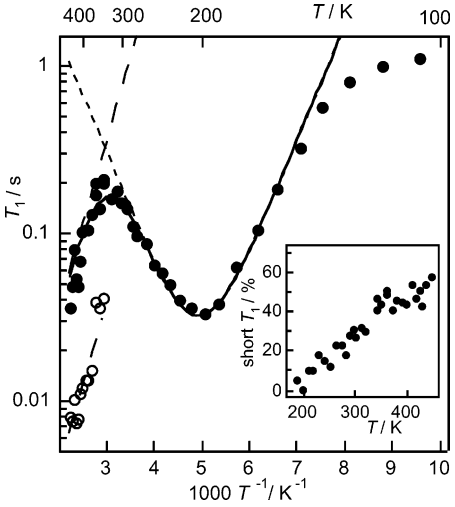

Figure 4. ^{1}H NMR spin−lattice relaxation times T_1 observed at 54.3 MHz for $(CH_3)_4N$−MC (M4−MC). Open and filled circles correspond to the shortest and longest T_1 values, respectively. Dotted and broken lines indicate calculated T_1 values for models of the C_3-rotation of four methyl groups and the cationic self-diffusion, respectively, and their superposition for the long component is shown by a solid line. The temperature dependence of the percentage of the short T_1 component is shown in the inset.

3.2.3. n-Butylammonium Ions in C41−MC and Tetramethylenediammonium Ions in C42−MC. The ^{2}H spectra observed in C41d_3−MC and C42d_6−MC given in Figure 5 show a typical Pake pattern. The QCC of 56 ± 1 kHz was obtained below 200 K in both C41d_3−MC and C42d_6−MC. This value agrees well with the calculated value of 58 kHz for the ND_3^+ rotation about its C_3-axis (ND_3^+-rot), indicating the onset of this motion below ca. 200 K.

The QCC values of C41d_3−MC and C42d_6−MC showed no remarkable reduction in the ranges 200−400 and 200−380 K, respectively, indicating that the cationic isotropic rotation which gives vanishing QCC is not excited.

In the ^{1}H T_1 measurement for C41−MC, the largest part of the magnetization recovery could be fitted by a single-exponential curve at 104 K. On the other hand, above 140 K the recoveries showed distributed T_1 values attributable to paramagnetic sites in the host. The short T_1 component became major above 300 K. T_1 values decreased monotonically above 250 K. Analogously to M3−MC and M4−MC, the T_1 behavior

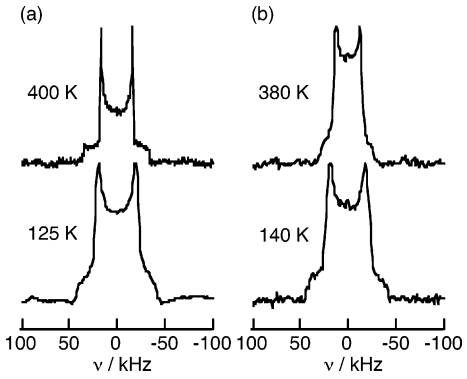

Figure 5. ^{2}H NMR spectra observed for (a) $CH_3(CH_2)_3ND_3-MC$ (C41d_3−MC) and (b) $ND_3(CH_2)_4ND_3-MC$ (C42d_6−MC).

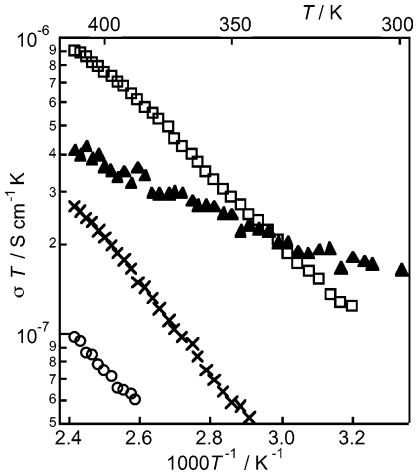

Figure 6. Temperature dependences of ac electrical conductivity, σ, measured at 1 kHz in $(CH_3)_3NH-MC$ (M3−MC, ▲), $(CH_3)_4N-MC$ (M4−MC, ○), $CH_3(CH_2)_3NH_3-MC$ (C41−MC, □), and $NH_3(CH_2)_4NH_3-MC$ (C42−MC, ×).

observed in C41−MC above 250 K was attributed to the excitation of the cationic 2-D self-diffusion, and then the longest and the shortest T_1 values were fitted with eqs 2 and 3. The estimated E_a is shown in Table 3.

In the T_1 measurement for C42−MC, a distributed T_1 was also observed above ca. 150 K and the percentage of the short T_1 component became major above ca. 250 K, suggesting that cationic 2-D self-diffusion is excited in C42−MC. The estimated E_a for 2-D diffusion is given in Table 3.

3.3. Cationic Self-Diffusion Measured by Electrical Conductivity. ac electrical conductivities measured with increasing temperature are shown in Figure 6. The $\ln(\sigma T)$ vs T^{-1} plots in each specimen showed a linear relation, indicating that the ionic conduction is thermally excited. Activation energies for the cationic 2-D self-diffusion were determined from the slopes of $\ln(\sigma T)$ vs T^{-1} plots by using the Nernst−Einstein relation, and are shown in Table 3. Conductivity and NMR measurements afforded an analogous trend in the E_a values.

3.4. Motional Properties of Small Alkylammonium Cations Located in the Interlayer Space of Tetrasilicicfluormica. In this study, the 2-D self-diffusion of small alkylammonium ions intercalated in tetrasilicicfluormica was detected. In C81−MC, where *n*-octylammonium ions form a densely packed cationic monolayer, the 2-D diffusion could not be observed in the ^{1}H T_1 up to 410 K.[7] It can be expected that the cationic 2-D diffusion becomes easy when many vacant hopping sites for cations are formed.

TABLE 4: Activation Energies (E_a) for Cationic Self-Diffusion in Bulk Crystals

compound	E_a/kJ mol^{-1}	ref
$(CH_3)_3NHBF_4$	21	12
$(CH_3)_4NSCN$	106	13
$CH_3(CH_2)_3NH_3Cl$	64	14
$NH_3(CH_2)_4NH_3Cl_2$	50	15

In Table 4, reported activation energies for the cationic self-diffusion in bulk crystals are listed. We can see that activation energies in the present intercalated compounds are lower than those in bulk crystals. This is because the density of anionic centers of mica layers is lower than that in bulk, resulting in enough space for small cations to diffuse in the interlayer space.

It is noted that the platelike trimethylammonium ion performs characteristic behavior; i.e., the 2-D self-diffusion takes place without the onset of the isotropic rotation in the interlayer space, whereas the cationic self-diffusion is always accompanied by the isotropic rotation in the 3-D system. This fact implies that the anisotropic orientations and molecular motions are favored in the 2-D space.

4. Conclusion

We observed the 2-D self-diffusion of alkylammonium ions in the interlayer space of tetrasilicicfluormica by solid-state NMR and ac conductivity measurements. This is the first observation of the cationic self-diffusion of organic species in clay compounds. In the ^{1}H NMR measurements, the 2-D self-diffusion could be recognized as the ^{1}H relaxation caused by the magnetic dipolar fluctuation between ^{1}H and paramagnetic spins. Activation energies for the cationic 2-D self-diffusion in the intercalation compounds were shown to be lower than those for the cationic diffusion in corresponding bulk crystals.

References and Notes

(1) Jacobson, A. J. In *Solid-State Chemistry Compounds*; Cheetham, A. K., Day, P., Eds.; Clarendon Press: Oxford, 1992; p 182.
(2) Lagaly, G. *Clay Miner*. **1981**, *16*, 1.
(3) Walker, G. F. *Clay Miner*. **1967**, *7*, 129.
(4) Davis, J. H.; Jeffrey, K. P.; Bloom, M.; Valic, M. F.; Higgs, T. P. *Chem. Phys. Lett*. **1976**, *42*, 390.
(5) Kobayashi, T.; Ohki, H.; Ikeda, R. *Mol. Cryst. Liq. Cryst*. **1994**, *257*, 279.
(6) Endo, T.; Sato, T.; Shimada, M. *J. Phys. Chem. Solids* **1986**, *47*, 799.
(7) Yamauchi, M.; Ishimaru, S.; Ikeda, R. *Z. Naturforsch., A* **1999**, *54*, 755.
(8) Hunt, M. J.; Mackay, A. L. *J. Magn. Reson*. **1974**, *15*, 402.
(9) Andrew, E. R.; Canepa, P. C. *J. Magn. Reson.* **1972**, *7*, 429.
(10) Abragam, A. *The principles of Nuclear Magnetism*; Oxford University Press: London, 1967.
(11) Solomon, I. *Phys. Rev*. **1955**, *99*, 559.
(12) Ishida, H.; Hayama, N.; Ikeda, R. *Chem. Lett*. **1992**, 1333.
(13) Tanabe, T.; Nakamura, D. *J. Chem. Soc., Faraday Trans.* **1991**, *87*, 987.
(14) Hattri, M.; Fukada, S.; Nakamura, D. *J. Chem. Soc., Faraday Trans.* **1990**, *86*, 3777.
(15) Iwai, S.; Ikeda, R.; Nakamura, D. *Can. J. Chem*. **1988**, *66*, 1961.